Combining *in situ* tribometry and triboscopy to understand third body behavior of a Cd coating

P. Behera, K. R. Sriraman, R. R. Chromik & S. Yue

Department of Mining & Materials Engineering

McGill University, Montreal, QC, Canada H3A 0C5

Abstract

The dynamic nature of third bodies and the buried nature of a sliding contact makes it difficult to interpret and correlate changes in the coefficient of friction to instantaneous materials changes. That is, full utilization of the 'tribological circuit' as proposed by Berthier, to describe tribological flows is often limited in practice unless specialized techniques are used. In this paper, an *in situ* tribometer is used to understand the evolution and flow of third bodies and their effect on the coefficient of friction. The *in situ* tribometer consisting of a transparent sapphire countersphere coupled with optical microscope is used to study the interface during linearly reciprocating sliding with simultaneous measurement of the coefficient of friction by measuring the tangential force with a time-resolved piezo sensor at a sampling rate of 800 Hz along the track length. This provides instantaneous coefficient of friction measurements along the localized track length, allowing one to plot 'spatial friction' maps, also known as triboscopic images. These graphs are cycle number on the x-axis and track position on the y-axis with a color coding for coefficient of friction. The *in situ* images of third bodies are correlated with the triboscopic images to identify third body flows and how they relate to local frictional changes. A soft coating (Cd) on hard substrate (low carbon steel) is used to study these third body phenomenon.

1 Introduction

Metallic surfaces in sliding contact occur often in industrial applications. More often than not, the contact is lubricated, but dry sliding is possible. Soft metallic coatings may act as solid lubricants and find applications requiring moderate reduction in friction and mitigation of 'running-in' wear [1]. Using the 'third body concept' proposed by Berthier [2], metallic coatings (first bodies) placed in sliding contact will lead to the formation of third bodies [2], which will influence the friction coefficient. Metallic coatings [3] may be used to reduce the friction and wear by modifying the velocity accommodation mechanism between the two first bodies [4]. Blau [5] postulated that the transfer of metal from one surface to the other changes the sliding characteristics and leads to changes in contact area, morphology of the materials and re-deposition of heterogeneous material from either of the first bodies.

Due to the nature of the buried interface for standard tribology testing, the dynamic nature of third body generation and its recirculation at the contact is difficult to understand and correlate with friction

coefficient changes. Real-time studies that can capture the physical and mechanical changes occurring at the interface, simultaneously recording and linking the friction coefficient to third body flows, requires *in situ* methods [6]. In situ and other real-time or "on-line" methods have been developed over the years. Monitoring of the electrical contact resistance and friction force with spatial sensors, often called 'triboscopy', allows one to correlate friction and third body activity to specific locations on the worn surface or to specific third body flows in the contact region [7]–[9]. An "on-line" tribometer, developed in the group of Dienwiebel [10] probes the worn surface (outside the contact) with a holographic microscope, allowing one to observe surface morphology changes that may correlate with the friction. *In situ* tribometry, using a transparent counterface, allows direct observation of the sliding interface and has been used to study third body formation and evolution for solid lubricants [11][12], composite coatings [13][14] and wear resistant coatings [6][15]. All of these techniques observe third bodies in different ways and are most effective when coupled with *ex situ* observations of worn surfaces by standard visual, morphological, chemical and mechanical characterization techniques [6]. Less frequently, these in situ methods are coupled with one another. Recently, Stoyanov et al. reported on a lubricated sliding contact for aluminum using both in situ and on-line tribometry [16].

While the in situ methods have been most often applied to solid lubricants[11], [17], [18], [19], there have been many recent studies on metals [16][10], [13], [20]–[27]. In the work of Sriraman et al. [20] they studied Low Hydrogen Embrittling (LHE) Cd coatings, which are relatively soft coatings applied on high strength steel for fasteners and landing gear components which withstand sliding motion during their application. The lubricous nature of the Cd [28] makes the coating further advantageous to be studied for its tribological behavior by third body formation. *In situ* studies by Sriraman et al. [20] on electroplated Cd coatings showed transfer film formation followed by recirculation of third bodies and finally removal of the transfer film. Jahanmir et al. [29] and Birkett et al. [30], using standard tribology testing, showed that the presence of 0.1 μm Cd coating on hard substrate reduces the wear rate in comparison to uncoated substrate materials.

In situ methods have helped understand third bodies at the sliding interface and their effect on the tribological properties in a way that is unobtainable by other methods. However, a common criticism is that the counterbody used in these studies (i.e. typically sapphire) are different from engineering applications and could affect somewhat the tribological behavior [31] and evolution of third bodies. As mentioned above, the buried interface may also be probed, in a somewhat different manner, utilizing triboscopic maps generated with a metallic countersphere. Belin et al. [8][7][9] used triboscopic maps to study the degradation of thin films by coupling cyclic tests with friction coefficient imaging showing increase in coefficient of friction as well as seizure of the coating. These studies showed a method to investigate the instantaneous variation in friction with respect to time and position and combine the average coefficient of friction with microscopic peculiarities at each point within the wear track. Though triboscopic maps are used to study coating degradation, it is most often combined with electrical contact resistance methods where a high electrical contact resistance is measured when the polymeric coating deposited on metallic substrate is intact and subsequent decrease in electrical contact resistance as the insulating polymeric coating is degraded with increase in sliding cycles, limiting the study only to non-metallic coating.

The current work focuses on studying the third body evolution by *in situ* tribometry and triboscopy, correlating the observations of dynamic nature of third bodies to the detailed analysis of time and spatially resolved friction maps from triboscopy. Friction maps generated for tests on coatings with steel countersphere were studied for third body evolution by an analysis of spectral features that could be tied to behavior observed by in situ tribometry. The tribological tests were carried out in a linearly reciprocating ball on flat surface with a sapphire countersphere to correlate the in situ studies with the triboscopic images and extend it to metallic countersphere by spectral analysis.

2 Experimental Methodology

2.1 Plating conditions and coating characterization

The Cd coating was plated in an industrial facility in an alkaline cyanide bath solution with CdO – 20-30 g/l, NaCN – 90-135 g/l, Na_2CO_3 – 0-60 g/l and NaOH – 11-30 g/l. The current density for plating was 118-120 mA/cm^2 to generate an average coating thickness of 15 µm. After coating, a trivalent chromate conversion coating was done to generate a passivation layer in nm range. The plating was done on 6" X 6" inch low carbon 1010 steel and baked at 200 ^{0}C for 24 hrs, the plates were then sheared into 1" X 1" inch coupons for tribological test.

SEM analysis of the surface and cross-section of the LHE Cd coating was done by Philips FEI Inspect F-50 instrument equipped with a field emission gun, operated at 20 kV for surface morphology and 10 kV for cross-section analysis at 2500X magnification.

The hardness of the coating and substrate was measured by nanoindentation technique using Hysitron triboindenter. The loading and unloading is done for 5 secs with a maximum force of 5000 µN and holding time of 2 secs at the maximum load using a calibrated Berkovich diamond indenter. The hardness of the coating and substrate was determined by using Oliver and Pharr analysis[32].

2.2 Tribological Test Parameters

The tribological tests were carried out with a linearly reciprocating ball on a flat tribometer [14]. For in situ tests, the counterface was a sapphire hemisphere (3.175 mm radius), while for standard tribology tests (blind test) a 440C steel countersphere (3.175 mm radius) was used. The average surface roughness of sapphire countersphere was 0.068 µm and average surface roughness of steel countersphere was 0.135 µm. The normal load applied to the contact was set with dead weights applied on the arm. For in situ test, 0.863 N was applied, while for standard testing 1.275 N was used. This led to an initial maximum Hertzian contact stress of 390 MPa for both type of tests. The friction force was measured with a piezoelectric sensor at a sampling rate of 800 Hz and a low-pass filter cutoff frequency 200Hz is used to attenuate noise form the measurement. The lateral resolution of the friction measurements was on the order of 20 µm, which was smaller than theoretical contact radius calculated according to Hertzian [33] two body contact theory (sapphire countersphere – 34.3 µm and steel countersphere – 33.1 µm). The coefficient of friction value was plotted as a color coded map as a function of track position and cycle number to generate what is often termed a "triboscopic image," [9] representing the spatial and temporal evolution of the friction coefficient. Friction versus position along the wear track for individual cycles was also plotted either as

the average friction calculated by averaging the instantaneous coefficient of friction from forward and backward directions or as 'instantaneous' friction coefficient, which is for either sliding direction (forward and backward direction) and unaveraged.

For in situ tests, a video camera with a pixel resolution of 853 X 480 at 29.97 frames per second, attached to an optical microscope with 10x optical zoom was used to record video of the contact through the sapphire hemispherical counterfaces and to study the third body evolution during the test. The video of the test is paused at the desired cycle number and track position and a snapshot was captured as an *in situ* micrograph.

The relative humidity during both the *in situ* test and blind test was maintained by passing dry air to the instrument enclosed within a plastic bag. The relative humidity for both of the test was kept at 0% RH which was assigned a designation of RH0. The track length for both of the test was 10 mm with a sliding velocity of 3 mm/s. The total number of cycles for *in situ* test was 1600 cycles leading to total sliding distance of 32 meters whereas for blind test the total number of cycles was 2000 cycles leading to a total sliding distance of 40 meters. Sampling rate and spatial resolution was the same for both *in situ* and blind test.

3 Results

3.1 Coating Characterization

The surface morphology of as-received LHE Cd coating (Figure 1(a)) consists of spherical platelets. The porous structure of this coating is necessary to allow hydrogen to escape during bake-out procedures required for high strength steel fasteners. The coating cross-section has non-uniform thickness (shown in Fig. 1(b)), with a top surface roughness due to the platelet morphology. The coating/substrate interface shows pockets of Cd filling the inherent roughness of the steel substrate. The coating has an average thickness of 11 ± 2 µm. The hardness of the coating measured on the cross-section of Cd coating is 0.42 ± 0.09 GPa, while the hardness of the steel substrate measured on un-coated steel substrate surface is 1.91 ± 0.06 GPa.

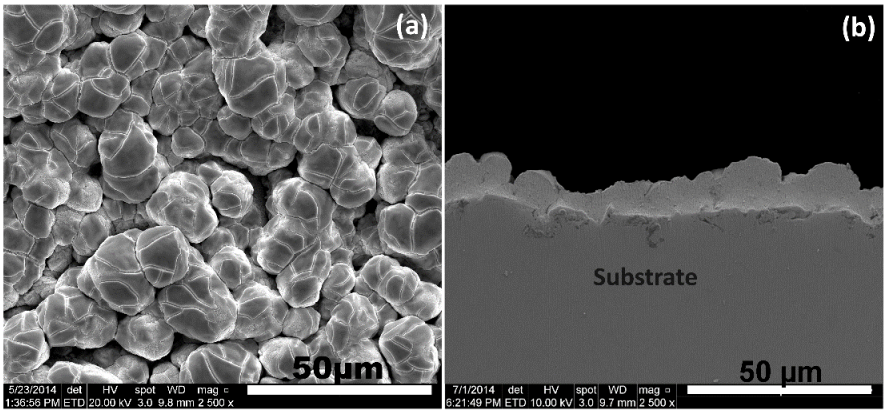

Figure 1 SEM Characterization of LHE Cd Coating (a) Surface Morphology, (b) Cross-section

3.2 In situ and Triboscopic Studies

As shown in Figure 2, Berthier [2] divided the flow of third bodies into five different types, encompassing the "tribological circuit". The detachment of materials from the first bodies to form third body is called as source flow (Q_s). The movement of third bodies across the interface is called as internal flow (Q_i). Third bodies ejected out from the contact region are called ejection flow (Q_e). The ejection flow can be reintroduced into the contact region leading to recirculation flow (Q_r) or can be permanently removed from the tribological circuit and become wear flow (Q_w) .

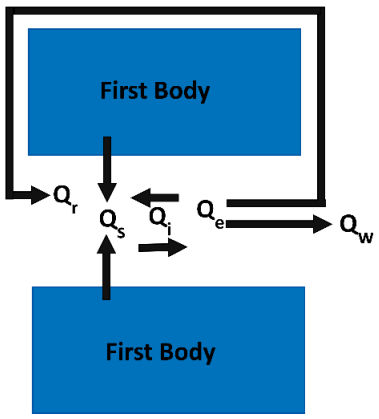

Figure 2 Tribological circuit by Berthier [1]

From the start of the tribological test, Cd coating acts as source flow (Q_s) for formation of third bodies. In situ micrographs showed formation of transfer film in the first cycle (see Fig. 3) by plastic flow [12] and adhesion of the coating due to its ductile characteristics. During early cycles as the test progresses, Q_s continues with increase in transfer film size at 10 cycles (see Figure 3) as compared to the first cycle. The transfer film area at 1 cycle is ~0.019 mm^2, which increases to ~0.041 mm^2 at 10 cycles (measured from Fig. 3). At cycle 1(run-in), the instantaneous coefficient of friction vs track position is predominantly higher than at 10 cycles. This is due to the adhesive transfer of the coating to the counterface and formation of the wear track, which is likely accompanied by ploughing of the rough coating by the sapphire countersphere. This process of shearing and adhesion of the metal is known as prow formation [34]–[36]. Eventually, as the transfer film grows and becomes more stable in size, the source flow, Q_s, subsides to some extent and the friction is reduced slightly.

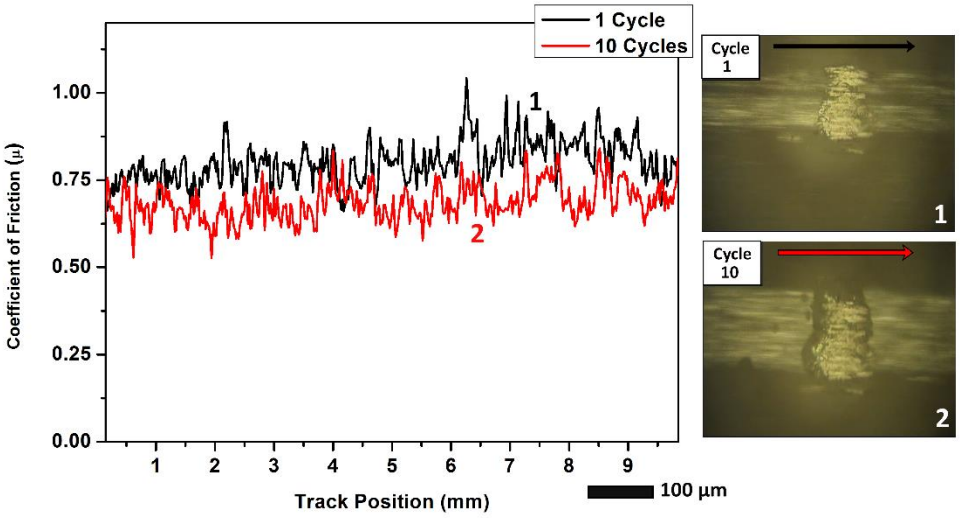

158

159 Figure 3 Coefficient of friction (averaged from forward and backward portion of given cycles) vs track
160 position with *in situ* image at 1 and 10 cycles indicating higher coefficient of friction due to prow
161 formation at 1 cycle which is subsequently lowered at 10 cycles due to decrease in prow formation

162 The instantaneous coefficient of friction in forward and backward direction vs track position is shown in
163 Fig. 4 at cycle 11. The appearance of the transfer film at point 1 (transfer film area ~0.039 mm^2) at 11 cycle
164 in forward direction is comparable to the transfer film area at cycle 10 (see Fig. 3), indicating transfer film
165 stability. However, during the backward sliding of the countersphere the transfer film becomes unstable
166 resulting in ejection and subsequent replenishment, which is a mix of Q_e and Q_s. At point 2 (see Fig. 4)
167 removal of transfer film (Q_e) leads to a sudden decrease in instantaneous coefficient of friction. After the
168 removal of transfer film, re-initiation of source flow (Q_s) in backward direction increases the instantaneous
169 coefficient of friction due to prow formation, marked as point 3 with corresponding micrograph.

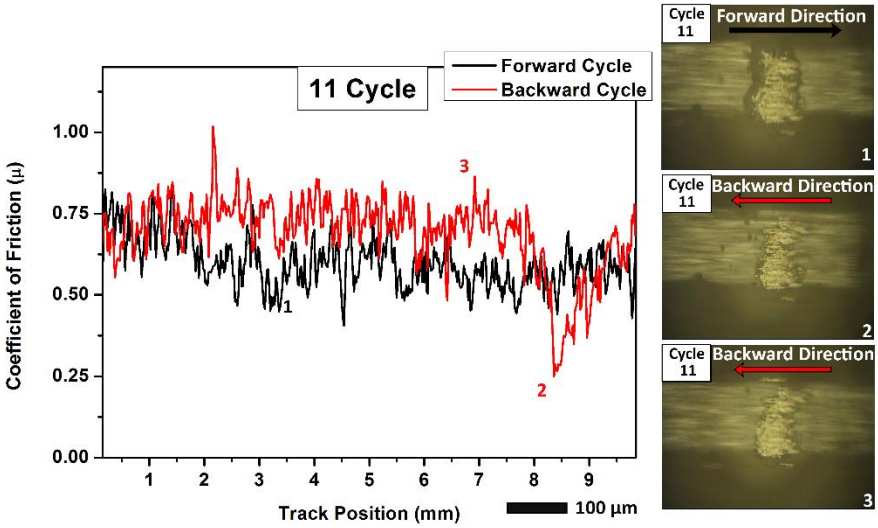

170

171 Figure 4 Instantaneous coefficient of friction vs track position with *in situ* image at 11 cycle, indicating
172 presence of transfer film at the contact interface in position 1, removal of transfer film at position 2 and
173 formation of new transfer film at position 3

As the test progresses, the transfer film becomes stable (transfer film area of 0.046 mm^2 - measured from Fig. 5) indicating a reduction in source flow (Q_s) similar to 10 cycle and 11 cycle (forward direction). At the end of the forward direction of the countersphere at 35 cycle shown in Fig. 5, attachment of small wear debris (2806 μm^2 in area) at the right edge of the contact region increases the instantaneous coefficient of friction. The small chunk is eventually ejected (Q_w) at the end of the forward direction shown as spike in the coefficient of friction. This phenomenon of ejection of wear debris particle at the end of the wear track occurs many times during the test but most of the features are buried within the interface and are difficult to observe from the *in situ* video. At cycle 35, this phenomenon is clearly observed and reported.

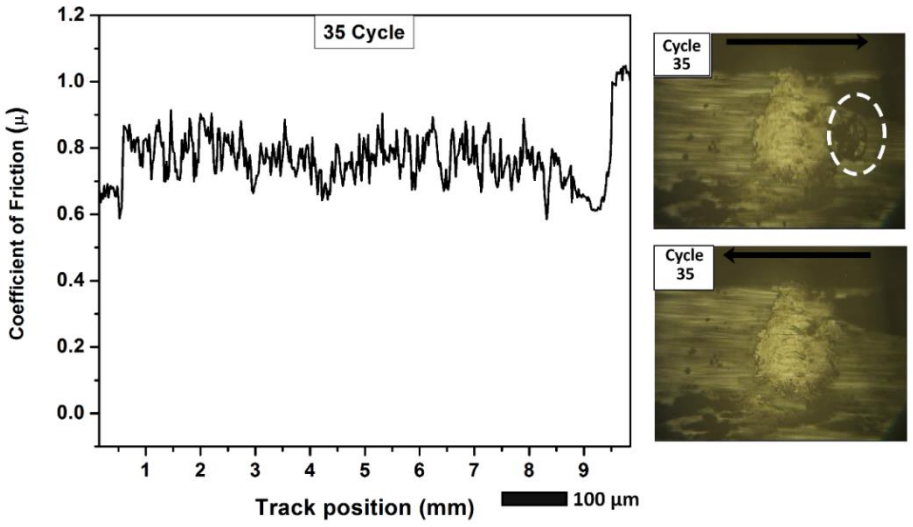

Figure 5 Coefficient of friction (averaged from forward and backward portion of given cycles) vs track position with *in situ* image at 35 cycle indicating recirculation of wear debris and subsequent ejection of wear debris observed at the end of wear track

At 46 and 49 cycle, adherence of wear debris at the end of the wear track is observed (See Fig. 6); this adherence increases the coefficient of friction at around 3.5mm till the end of the wear track due to increase in contact area. The coefficient of friction at point 2 is relatively higher than at point 1, the adherence of wear debris at point 2 leads to increase in coefficient of friction as compared to point 1. Though point 1 has coefficient of friction relatively lower than point 2, point 1 has higher instantaneous coefficient of friction than at 3.5 mm, this might be due to adherence of wear debris that is not revealed in the *in situ* micrograph.

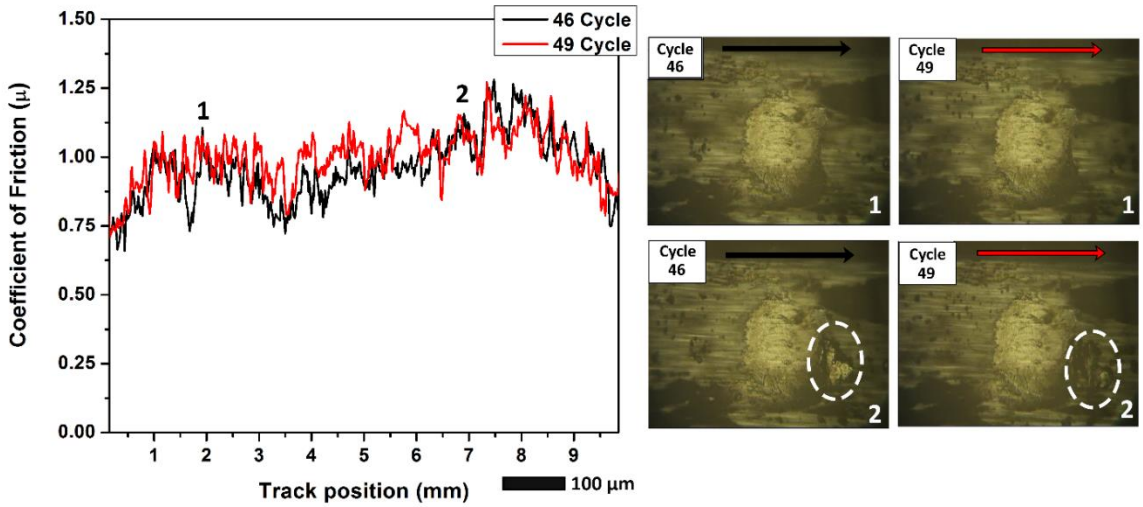

Figure 6 Coefficient of friction (averaged from forward and backward portion of given cycles) vs track position with *in situ* image at 46 cycle and 49 cycle indicating adherence of the wear debris, increasing the coefficient of friction at position 2 as compared at position 1 with additional attachment of wear debris.

Localized increase in coefficient of friction leads to increase in average coefficient of friction at 271 cycle, shown in Fig. 7. The contact region increases at 271 cycle due to attachment of third body to the countersphere at the top part of the *in situ* micrograph (see Fig. 7, 271 Cycle). This third body has particulate morphology indicating extruded third body reintroduced into the contact region and hence was attributed to recirculation flow, Q_r. At 283 cycle, the removal of this extruded third body decreases the average coefficient of friction as shown in the *in situ* micrograph.

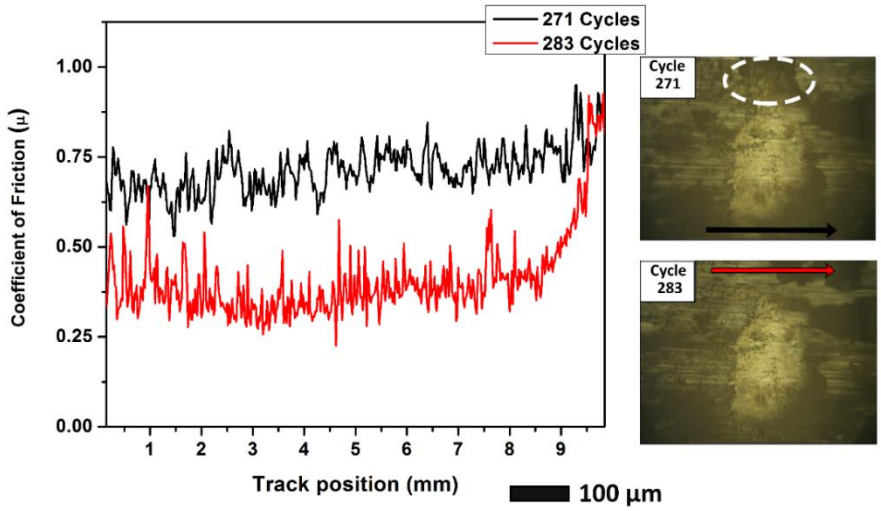

Figure 7 Coefficient of friction (averaged from forward and backward portion of given cycles) vs track position with *in situ* image at 271 and 283 cycles indicating the increase in coefficient of friction with adherence of additional transfer film at 271 cycle and subsequent decrease in coefficient of friction as the transfer film is removed at 283 cycles.

To summarize the instantaneous coefficient of friction associated with third bodies up to 300 cycles at RH0, triboscopic image is plotted in Fig. 8. At initial cycles, the high coefficient of friction due to prow formation by source flow (Q_s) at 1 cycle can be identified from the triboscopic image, which subsequently stabilizes to a relatively lower coefficient of friction at 10 cycles. With further progress of the test, the transfer film is removed and a new transfer film is formed by Q_s at 11 cycles. This removal of the wear debris by Q_w also leads to a friction coefficient change identified by the triboscopic image. The wear debris attached at the contact region (at 46 cycles) increases the instantaneous coefficient of friction as seen in triboscopic image, the continuation of similar features for next 20 cycles at the same track position indicates recirculation flow (Q_r). The average coefficient of friction as shown in Fig. 7 at 271 cycles is higher as compared at 283 cycles, this is due to modified contact condition by attachment of extruded third body at the contact region. This vertical features thus formed during the test (see Fig. 8 at 271 cycle) is due to intermittent attachment of third body at the interfacial contact region (it is difficult to identify all the vertical features due to limitation in resolution of optical microscope and transfer films obscuring the visibility of third body for every vertical features in the test).

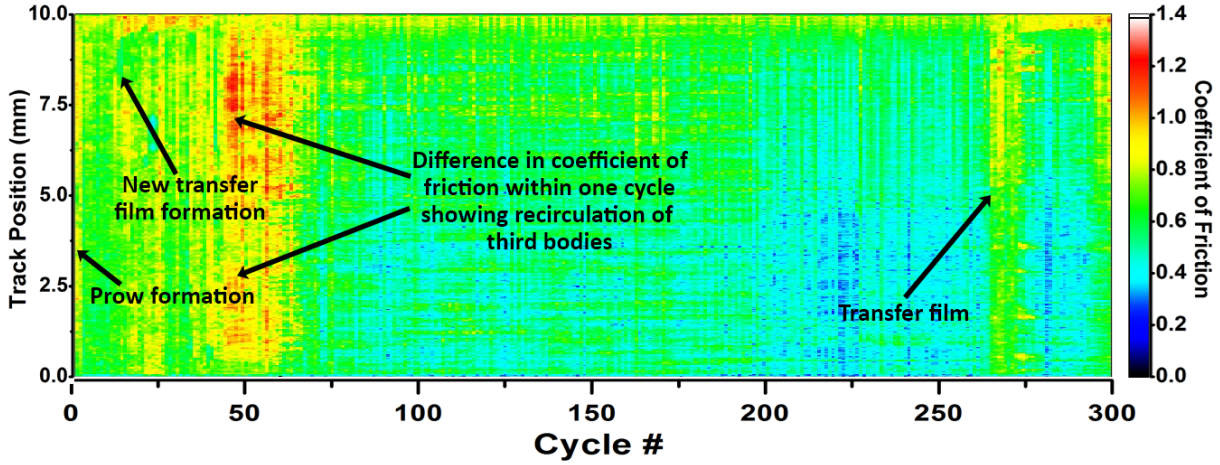

Figure 8 Triboscopic image summarizing the change in friction coefficient with morphological changes at the contact region observed by *in situ* tribometry. Prow formation as observed in Figure 3, new transfer film formation as observed in Figure 4, recirculation flow observed in Figure 6 and transfer film formed by extruded product as observed in Figure 7.

The triboscopic image up to 1600 cycles overlapped with a plot of the average coefficient of friction is presented in Fig. 9(a). Information later in the test is often more difficult to observe due to a thick and stable transfer film. However, at cycle 1100 (see Fig. 9 (b)) holes and scoring marks on the transfer film are seen. The hole is replenished after few cycles indicating source flow (Q_s) with additional attachment of transfer film at the bottom (shown as recirculation flow in Fig. 9(c)). Though the bulk layer of Cd coating might have been removed, the presence of Cd coating at the islets of the steel substrate acts as reservoir for the replenishment of the third body. The scoring of the transfer film (categorized as horizontal scratched regions on the transfer film) increases as shown in Fig. 9(b) and Fig. 9(c); the transfer film is completely removed at the end of the test (1599 cycle) leading to decreased occurrence of vertical features as seen from the triboscopic image and *in situ* micrograph at the end of test. The average

instantaneous coefficient of friction plotted at 1520 and 1599 cycles is shown in Fig. 9(d). The *in situ* micrograph indicates that even though there is transfer film present, the instantaneous coefficient of friction vs track position at 1520 and 1599 cycles have peaks at relatively same track position indicating predominant wear track morphology effect as compared to morphological changes associated with transfer film.

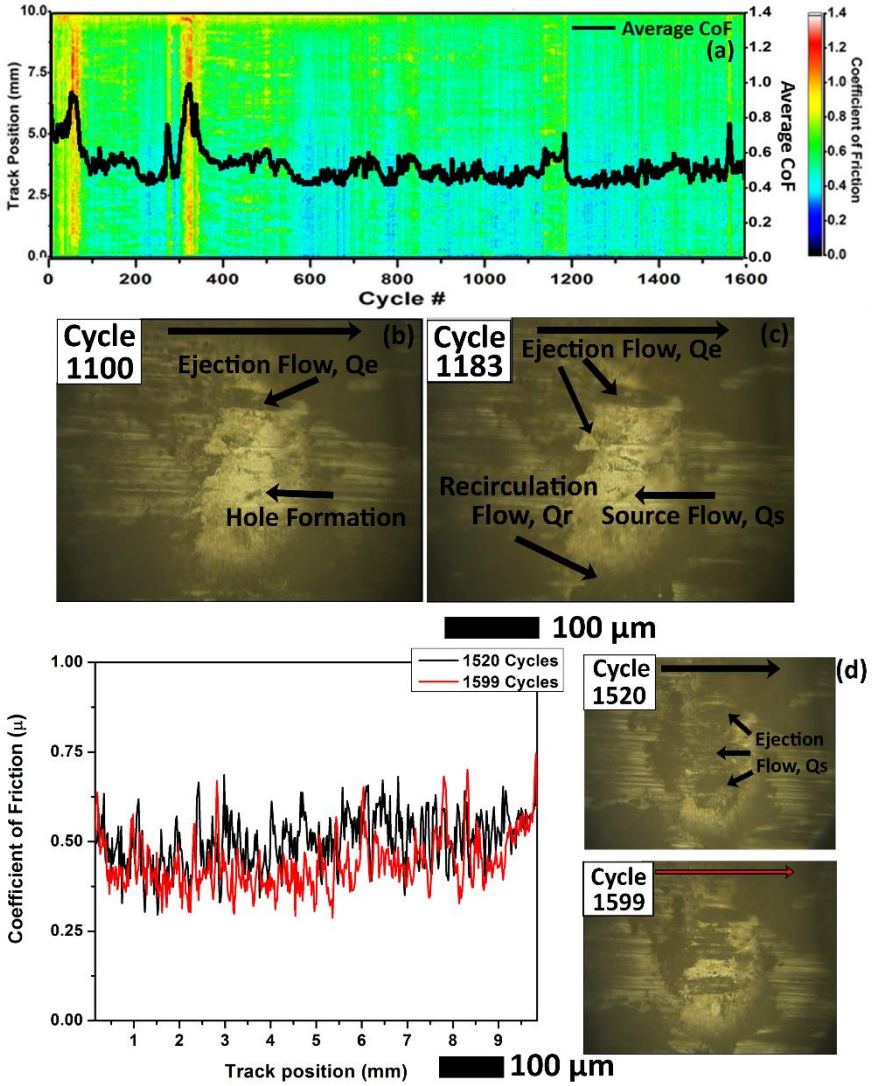

Figure 9 (a) Average coefficient of friction superimposed on triboscopic image of the full test, in situ micrograph at (b) 1100 cycles indicating scoring marks and hole formation on the transfer film, (c) 1183 cycles indicating replenishment of some previously formed holes, increasing in scoring and additional transfer film attachment at the contact interface, (d) Coefficient of friction (averaged from forward and backward portion of given cycles) vs track position at 1520 and 1599 cycles showing removal of transfer film and predominant effect of wear track morphology

3.3 Triboscopy with steel counterbody (Blind test)

For comparisons to in situ tribology, a more 'traditional' countersphere of AISI 440C steel was used for tribological testing of the Cd coating at RH0. The results from *in situ* microgrpahs correlated with the triboscopic images in the previous section were used as a basis to understand the triboscopy for the blind tests. Similar behavior as seen in case of *in situ* triboscopic studies are also seen in blind test (from triboscopic images). The initial overall high instantaneous coefficient of friction at 5 cycles (shown in Fig. 10) as compared to 8 cycles is due to prow formation. With further progress of test, the high coefficient of friction at 27 cycles than 8 cycles is due to change in contact conditions by formation of transfer film by source flow (Q_s). The change in instantaneous coefficient of friction before and after 5 mm of track length at 52 cycles is similar to the features seen at 45 cycles form *in situ* studies (see Fig. 6) indicating attachment of wear debris (recirculation flow, Q_r) at the contact region.

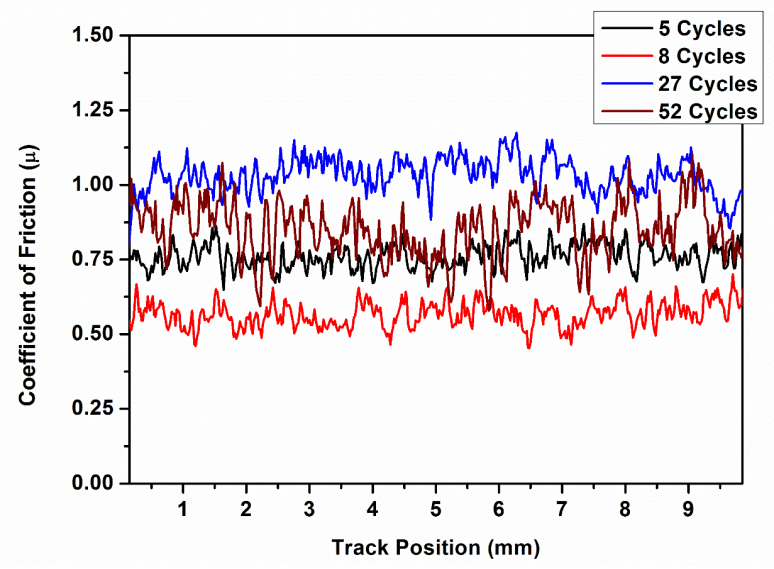

Figure 10 Coefficient of friction (averaged from forward and backward portion of given cycles) vs track position at cycle 5, 8, 27 and 52 indicating change in coefficient of friction with progress of test.

Triboscopic image with steel countersphere is plotted up to 300 cycles as shown in Figure 11. Features that were similar to Fig. 8 are identified and demarcated. Feature 1 similar to prow formation in Fig. 8 is shown in Fig. 11, this feature was observed at higher number of cycles as compared to sapphire countersphere. Feature 2 is similar to new transfer film formation by source flow (Q_s). Wear debris attachment seen in Fig. 9 is also observed with steel countersphere in feature 3. New transfer film formation by extruded third bodies from the contact region observed at 271 cycles for *in situ* test can be demarcated as Feature 4 from Fig. 11.

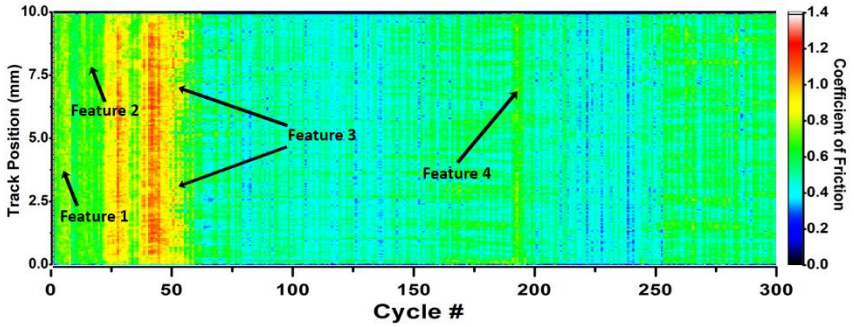

Figure 11 Triboscopic image of blind test up to 300 cycles to observe features similar to *in situ* test

The average coefficient of friction overlapped with triboscopic image up to 2000 cycles for blind test is shown in Fig. 12. Average coefficient of friction overlapped with the triboscopic image shows an initial spike in friction coefficient to 1.0 which is similar for both *in situ* test and blind test. Stable regime of coefficient of friction at approx. 0.5 approx. is similar for both *in situ* test and blind test. Dsicrete vertical features seen at 70 cycles for *in situ* triboscopic image is similar to features seen at 50 cycles for blind test. Morphological changes like initial run-in period, transfer film formation, attachment of wear debris and attachment of additional extruded transfer film occurring at the contact region leading to change in spatial and temporal changes in the friction coefficient for *in situ* test can also be correlated with the blind-test by comparing the triboscopic image.

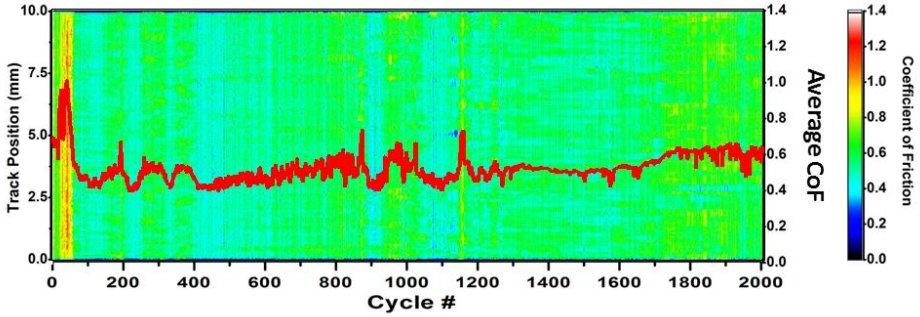

Figure 12 Triboscopic image overlapped with average coefficient of friction showing sudden increase in average coefficient of friction due to formation of third bodies at the contact region with steel countersphere at RH0

3.4 Spectral analysis of *in situ* and blind test

Specific correlations between triboscopic images are difficult by simple inspection, thus a 'spectral' analysis was carried out where the distribution of measure friction coefficients over a certain range of cycles is plotted. Comparison of the spectral analysis of the instantaneous friction data for sapphire (*in situ*) and steel (blind test) countersphere helps to ascertain the extent to which similarities exist in friction trends. Regions studied for spectral analysis were typically features that were stable over a given range. These could be regions of relatively constant friction across the wear track or regions where there are intermittent changes across the track. The analysis was carried out over a range until some abrupt increase and decrease of average coefficient of friction occurred, signaling some change in the contact

and/or wear track conditions. A relative frequency distribution of the instantaneous coefficient of friction was done with a binning of 0.05 and a bar chart was plotted to comprehend different vertical features.

Discrete vertical features associated with wear debris attachment at the contact region for short no. of cycles is identified from *in situ* and blind test (see figure 13). The features from the triboscopic image are analyzed for similarity in relative frequency distribution of instantaneous coefficient of friction. At cycle 37-69 for *in situ* test (see Fig. 6) and 18-63 for blind test has instantaneous frequency distribution between 0.4 and 1.1 and maxima at 0.9 due to Q_s and Q_r of the bulk layer of the coating. The distribution of relative frequency at cycle 263-282, 517-560, 674-772 for *in situ* test is due to formation of transfer film from the extruded Cd coating ejected from the contact region during the tribological test (see Fig. 7), this relative frequency distribution is similar for blind test at 188-196 and 859-875 cycles. The initiation of scoring mark and holes with depletion of transfer film by ejection flow (Q_e) observed around 1100 cycles for *in situ* test with subsequent replenishment of the holes and scoring marks leads to increase in average coefficient of friction. For *in situ* test at 1123-1193 and 1552-1572 cycles the replenishment of the holes and attachment of additional transfer film (see Fig. 9(c)) shows an instantaneous frequency coefficient of 0.55-0.6 maxima which is comparable to relative frequency distribution at 1144-1160 cycles for blind test.

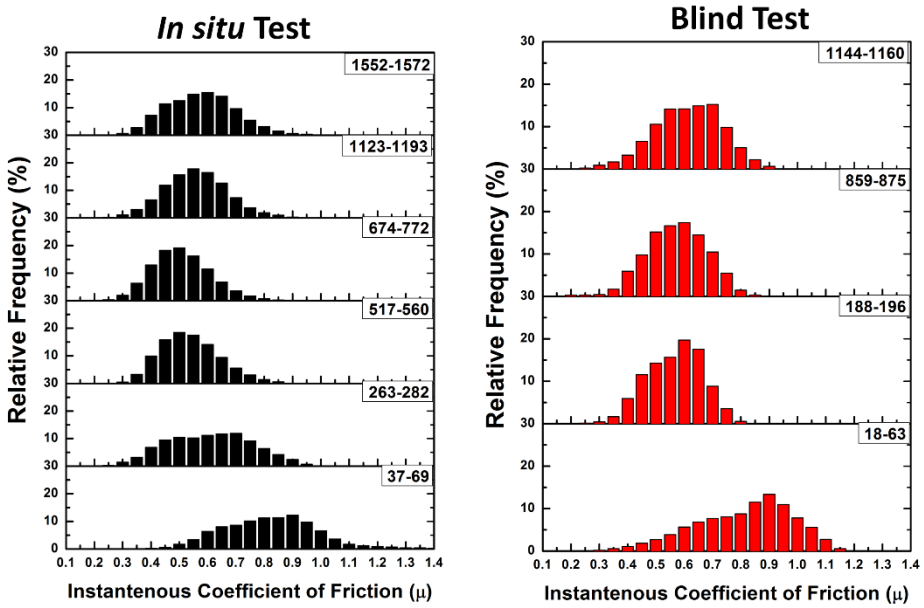

Figure 13 Relative frequency distribution of vertical features identified from the triboscopic image of *in situ* and blind test with selected range of cycle number indicated at top right corner of each plot

Regions with mix of vertical and horizontal features identified from the triboscopic image (see Fig. 14) are analyzed for similarity in relative frequency distribution between *in situ* test and blind test. Relative frequency distribution at cycle 490-503 shows a more uniform distribution of instantaneous coefficient of friction as compared at 254-313 for blind test, but the maxima for both of the relative frequency distribution is at 0.55-0.6 indicating similarity in the third body morphology. Features analyzed for relative

frequency distribution for *in situ* test at 768-794 and 851-908 cycles compared to blind-test at cycle 891-940 and 1045-1138 is similar indicating similar behavior of third bodies at the contact region during sliding. Similar relative frequency distribution is also observed at cycle at 798-848 for *in situ* test compared to relative frequency distribution for blind test at cycle 941-988 cycle. Relative frequency distribution at cycle 934-986 for *in situ* test is also similar to features analyzed at cycle 1306-1384 for blind test. The overall similarity between the *in situ* test and blind test for relative frequency distribution of instantaneous coefficient of friction for similar features identified from the triboscopic image indicates similar behavior of the third bodies. Thus the morphological changes in the third bodies identified from the combination of *in situ* image with the triboscopy can be extended to the blind test to identify the evolution of third bodies.

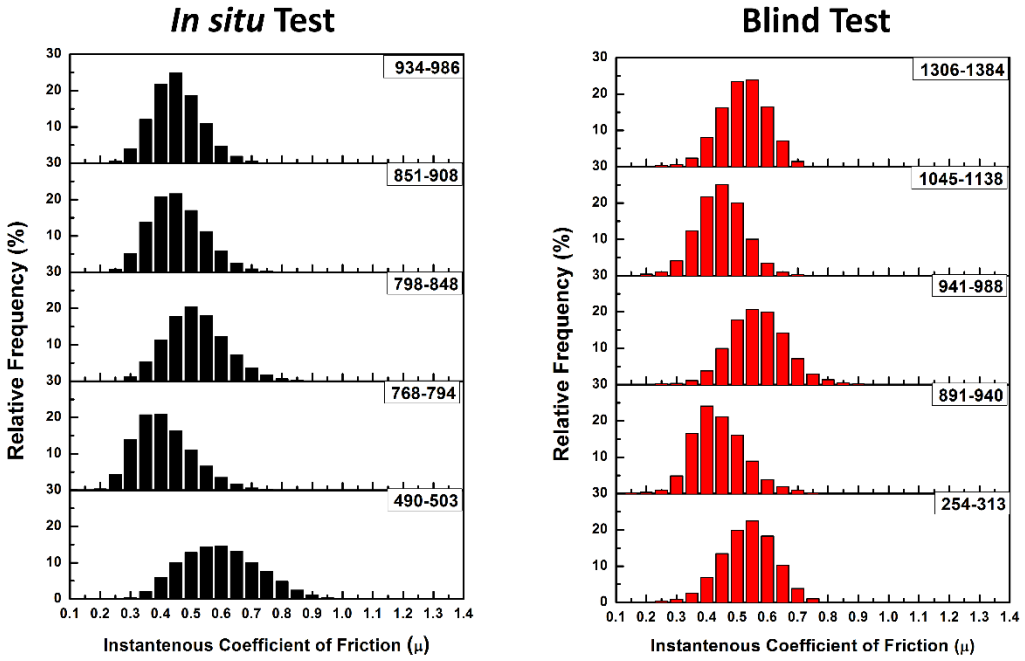

Figure 14 Relative friction coefficient frequency distribution of similar features identified from *in situ* and blind test with selected range of cycle number indicated at top right corner of each plot

4 Discussion

Dry sliding of a Cd coating was studied by *in situ* tribometry. Metal transfer films form in early cycles and persist for most of the test. While the opaqueness of these films prevent observation directly at the sliding interface, the size and morphology of the transferred material can be monitored to determine some information about third body flows. The transfer film formed at 1 cycle of the test increases in size as the test progresses, the transfer film thus formed by source flow is removed stochastically with formation of new transfer film immediately with new source flow. Attachment of wear debris and recirculation of wear debris at the contact region, formation of hole and scoring mark on the transfer film is also observed by *in situ* tribometry. Similar behavior of third body flow at the contact region like transfer film formation, its instability and subsequent removal was also observed by Sriraman et al.[20]. Increase in average

coefficient of friction with formation of transfer film due to plastic flow, instability of transfer film and its healing for soft Al coating similar to current study is also observed by Shockley et al.[13]. Phenomenon of prow formation by activation of source flow and recirculation of the third bodies, intermittent occurrence of internal flow and ejection flow was also observed by Shockley at al.[37] for cold sprayed Al coating.

While many of the third body flows for metals were observed previously, this study was the first to make direct correlations between these in situ observations and measurements of the spatial friction by triboscopy. Third body formation and changes to third body morphology at the contact region can significantly alter the instantaneous coefficient of friction leading to a subsequent change in average coefficient of friction. The formation of third bodies, its morphological change and circulation in the tribological circuit can be correlated with change in instantaneous coefficient of friction values leading to distinctive features in triboscopic image. The formation of transfer film associated with plastic flow and adhesion was associated with high coefficient of friction (see Fig. 3). Removal of the transfer film was often associated with a drop in coefficient of friction at the particular track position followed by increase in coefficient of friction due to prow formation (see Fig. 4). The attachment of wear debris at the contact region is associated with a mix of high and low coefficient of friction occurring for a few cycle as vertical feature with discontinuous color coding (see Fig. 7). These triboscopic features are also observed by Belin et al. [8] during initial run-in and ploughing of polymeric varnish coating of graphite powder coating on AS12UN coating showing continuous horizontal features (reversed axis - X-axis corresponds to number of cycles and Y-axis as position in this study) indicating high average coefficient of friction, further confirmed with electrical contact resistance method. Constant replenishment of the third bodies can be correlated to Cd acting as reservoir of solid lubricant [38] as shown by Belin et al. [9] with degradation of thin films with localized pockets acting as reservoirs to avoid decohesion and seizure of the coating.

Relative frequency distribution of similar features identified from *in situ* test and blind test shows similar trends indicating some similarity in third body flow at the contact region. Though the dynamic nature of the tribologial test leads to different features formed at different cycle no. for each type of test, the similarity in relative frequency distribution might be attributed to similar behavior of Cd coating at same relative humidity and contact stress with less dependancy on counterspheres used. Thus relative frequency distribution or spectral analysis is a useful method to correlate the third body flow for tests performed with different tribological parameters. While this was the case for sapphire and steel versus a Cd coating, future work on other material systems would be sure to reveal instances where the counterface materials strongly influence the tribological behavior.

In situ tribometry coupled with triboscopic image used in this study provided unique way to understand the dynamic behavior of third body flow at the contact interface. The *in situ* micrographs correlated with the signature instantaneous coefficient of friction can be extended to different counterspheres and different tribological parameter combined with spectral analysis. However, the formation of extensive transfer film can also obscure the interface leading to omission of some of the third body flow occurring at the buried interface. This is why in this study, specific correlations were presented but other interesting features on the triboscopic images were not fully explored. That is, often a friction change may occur but there is no direct correlation to something observable by in situ tribometry. The 'buried' interface problem remains for metals tribology as even with powerful in situ methods processes and third body flows directly

at the interface are often unobservable. Despite these difficulties in interlinking all the third body morphological changes with frictional changes at the interface, this study was useful in demonstrating the usefulness and effectiveness of a combined *in situ* and triboscopy study.

5 Conclusion

The current study helps in better understanding the dynamic nature of third bodies formed at the sliding interface and its subsequent effect on change in coefficient of friction. Combining *in situ* with triboscopic image helped in identifying the signature change in coefficient of friction with change in third body morphology at the interface. Spectral analysis of the specific features identified from the triboscopic image also revealed a correlation between tribological test performed with different counterspheres.

Tribological test performed on LHE Cd coating using *in situ* method revealed higher coefficient of friction during initial run-in period, removal of stable transfer film leads to sudden drop in coefficient of friction followed by increase in coefficient due to initiation of new source flow. Attachment of wear debris at intermittent positions on the wear track by recirculation flow increases the instantaneous coefficient of friction, specific to the track position. The effect of third body morphology at the sliding interface is also revealed from the triboscopic image; the change in coefficient of friction associated with change in third body morphology present at the interface can be identified from distinct features formed on the triboscopic image. Triboscopic image generated with steel counterspheres revealed similar features as identified from *in situ* triboscopic image indicating similarity in third body flow at the interface. Spectral analysis of the distinct features identified from the triboscopic image indicates change in third morphology with progress of test. Spectral analysis also helped in understanding the similarity in third body morphology with change in countersphere from sapphire to steel.

Combing *in situ* method with triboscopic image helped in linking the third body flow at the interface with distinctive features formed on the triboscopic image. The evolution of coefficient of friction also depends on other factors like change in chemical morphology and roughness of the third bodies which can be identified by combining other characterization technique like Raman spectroscopy, FT-IR spectroscopy and interferometry (on-line tribometry) coupling with *in situ* tribometry. The obscuring of the interface by formation of transfer film also limits the identification of features formed on the triboscopic image coupled with *in situ* tribometry which can be identified with better resolution of the interface.

Acknowledgments

The authors are thankful to Lisa Lee and Salim Brahimi for their support and inputs for this work. We would also like to thank Natural Science and Engineering Research Council Canada (NSERC), Boeing Research and Technology, Pratt & Whitney Canada, Héroux Devtek, Canadian Fastener Institute and Messier-Bugatti-Dowty for their financial support and for providing samples.

References

[1] K. Holmberg and A. Matthews, *Coatings Tribology: Properties, Mechanisms, Techniques and Applications in Surface Engineering*. Elsevier, 2009.

[2] Y. Berthier, "Maurice Godet's Third Body," in *Tribology Series*, vol. 31, C. M. T. D. Dowson T. H. C.Childs, G.Dalmaz, Y.Berthier, L.Flamand, J. M.Georges and A. A.Lubrecht, Ed. Elsevier, 1996, pp. 21–30.

[3] K. Holmberg, "A concept for friction mechanisms of coated surfaces," *Surf. Coat. Technol.*, vol. 56, no. 1, pp. 1–10, Dec. 1992.

[4] Y. Berthier, M. Godet, and M. Brendle, "Velocity Accommodation in Friction," *Tribol. Trans.*, vol. 32, no. 4, pp. 490–496, Jan. 1989.

[5] P. J. Blau, "Mechanisms for transitional friction and wear behavior of sliding metals," *Wear*, vol. 72, no. 1, pp. 55–66, Oct. 1981.

[6] R. R. Chromik, H. W. Strauss, and T. W. Scharf, "Materials Phenomena Revealed by In Situ Tribometry," *JOM*, vol. 64, no. 1, pp. 35–43, Feb. 2012.

[7] M. Belin, "Triboscopy: A new quantitative tool for microtribology," *Wear*, vol. 168, no. 1–2, pp. 7–12, Sep. 1993.

[8] M. Belin, J. Lopez, and J. M. Martin, "Triboscopy, a quantitative tool for the study of the wear of a coated material," *Surf. Coat. Technol.*, vol. 70, no. 1, pp. 27–31, Nov. 1994.

[9] M. Belin and J. M. Martin, "Triboscopy, a new approach to surface degradations of thin films," *Wear*, vol. 156, no. 1, pp. 151–160, Jul. 1992.

[10] S. Korres and M. Dienwiebel, "Design and construction of a novel tribometer with online topography and wear measurement," *Rev. Sci. Instrum.*, vol. 81, no. 6, p. 63904, Jun. 2010.

[11] I. L. Singer, S. D. Dvorak, K. J. Wahl, and T. W. Scharf, "Third body processes and friction of solid lubricants studied by in situ optical and raman tribometry," in *Tribology Series*, vol. 40, M. P. G. D. and A. A. L. D. Dowson, Ed. Elsevier, 2002, pp. 327–336.

[12] S. Descartes and Y. Berthier, "Rheology and flows of solid third bodies: background and application to an MoS1.6 coating," *Wear*, vol. 252, no. 7–8, pp. 546–556, Apr. 2002.

[13] J. M. Shockley *et al.*, "In situ tribometry of cold-sprayed Al-Al2O3 composite coatings," *Surf. Coat. Technol.*, vol. 215, pp. 350–356, Jan. 2013.

[14] H. W. Strauss, R. R. Chromik, S. Hassani, and J. E. Klemberg-Sapieha, "In situ tribology of nanocomposite Ti-Si-C-H coatings prepared by PE-CVD," *Wear*, vol. 272, no. 1, pp. 133–148, 2011.

[15] T. W. Scharf and I. L. Singer, "Role of third bodies in friction behavior of diamond-like nanocomposite coatings studied by In Situ tribometry," *Tribol. Trans.*, vol. 45, no. 3, pp. 363–371, 2002.

[16] P. Stoyanov, J. M. Shockley, M. Dienwiebel, and R. R. Chromik, "Combining in situ and online approaches to monitor interfacial processes in lubricated sliding contacts," *MRS Commun.*, pp. 1–8, Sep. 2016.

[17] I. L. Singer, S. D. Dvorak, K. J. Wahl, and T. W. Scharf, "Role of third bodies in friction and wear of protective coatings," *J. Vac. Sci. Technol. A*, vol. 21, no. 5, pp. S232–S240, Sep. 2003.

[18] K. J. Wahl, D. N. Dunn, and I. L. Singer, "Wear behavior of Pb–Mo–S solid lubricating coatings," *Wear*, vol. 230, no. 2, pp. 175–183, May 1999.

[19] R. R. Chromik, C. C. Baker, A. A. Voevodin, and K. J. Wahl, "In situ tribometry of solid lubricant nanocomposite coatings," *Wear*, vol. 262, no. 9–10, pp. 1239–1252, Apr. 2007.

[20] K. R. Sriraman *et al.*, "Tribological behavior of electrodeposited Zn, Zn–Ni, Cd and Cd–Ti coatings on low carbon steel substrates," *Tribol. Int.*, vol. 56, pp. 107–120, Dec. 2012.

[21] K. R. Sriraman, P. Manimunda, R. R. Chromik, and S. Yue, “Effect of crystallographic orientation on the tribological behavior of electrodeposited Zn coatings,” *RSC Adv.*, vol. 6, no. 21, pp. 17360–17372, Feb. 2016.
[22] J. M. Shockley, S. Descartes, P. Vo, E. Irissou, and R. R. Chromik, “The influence of Al2O3 particle morphology on the coating formation and dry sliding wear behavior of cold sprayed Al–Al2O3 composites,” *Surf. Coat. Technol.*, vol. 270, pp. 324–333, May 2015.
[23] Y. Zhang, J. M. Shockley, P. Vo, and R. R. Chromik, “Tribological Behavior of a Cold-Sprayed Cu–MoS2 Composite Coating During Dry Sliding Wear,” *Tribol. Lett.*, vol. 62, no. 1, p. 9, Feb. 2016.
[24] Y. Zhang, N. Brodusch, J. Michael Shockley, R. Gauvin, and R. R. Chromik, “Sliding-induced Microstructure of Cold-Sprayed Copper Coating Observed by Electron Channeling Contrast Imaging,” *Microsc. Microanal.*, vol. 20, no. Supplement S3, pp. 2104–2105, Aug. 2014.
[25] L. Lee, É. Régis, S. Descartes, and R. R. Chromik, “Fretting wear behavior of Zn–Ni alloy coatings,” *Wear*, vol. 330–331, pp. 112–121, May 2015.
[26] P. Stoyanov, R. R. Chromik, D. Goldbaum, J. R. Lince, and X. Zhang, “Microtribological Performance of Au–MoS2 and Ti–MoS2 Coatings with Varying Contact Pressure,” *Tribol. Lett.*, vol. 40, no. 1, pp. 199–211, Jul. 2010.
[27] P. Stoyanov, R. R. Chromik, S. Gupta, and J. R. Lince, “Micro-scale sliding contacts on Au and Au-MoS2 coatings,” *Surf. Coat. Technol.*, vol. 205, no. 5, pp. 1449–1454, Nov. 2010.
[28] V. Stepina and V. Vesely, *Lubricants and Special Fluids*. Elsevier, 1992.
[29] S. Jahanmir, E. P. Abrahamson II, and N. P. Suh, “Sliding wear resistance of metallic coated surfaces,” *Wear*, vol. 40, no. 1, pp. 75–84, Oct. 1976.
[30] A. Birkett and J. K. Lancaster, “Counterface effects on the wear of a composite dry-bearing liner,” *Wear*, vol. 110, no. 3–4, pp. 345–357, Aug. 1986.
[31] R. Ramadoss *et al.*, “Tribological properties and deformation mechanism of TiAlN coating sliding with various counterbodies,” *Tribol. Int.*, vol. 66, pp. 143–149, Oct. 2013.
[32] W. c. Oliver and G. m. Pharr, “An improved technique for determining hardness and elastic modulus using load and displacement sensing indentation experiments,” *J. Mater. Res.*, vol. 7, no. 6, pp. 1564–1583, 1992.
[33] K. L. Johnson, *Contact Mechanics* (Cambridge University Press), 1985.
[34] M. Cocks, “Interaction of Sliding Metal Surfaces,” *J. Appl. Phys.*, vol. 33, no. 7, pp. 2152–2161, Jul. 1962.
[35] M. Antler, “Processes of metal transfer and wear,” *Wear*, vol. 7, no. 2, pp. 181–203, Mar. 1964.
[36] M. Antler, “Wear, Friction, and Electrical Noise Phenomena in Severe Sliding Systems,” *E Trans.*, vol. 5, no. 2, pp. 297–307, Jan. 1962.
[37] J. M. Shockley, S. Descartes, E. Irissou, J.-G. Legoux, and R. R. Chromik, “Third Body Behavior During Dry Sliding of Cold-Sprayed Al-Al2O3 Composites: In Situ Tribometry and Microanalysis,” *Tribol. Lett.*, vol. 54, no. 2, pp. 191–206, Apr. 2014.
[38] Z. Rymuza, Ed., “3. Lubricants,” in *Tribology Series*, vol. 13, Elsevier, 1989, pp. 33–72.